2016-08-16

Current whole-body MRI applications in the neurofibromatoses

Ahlawat, S

http://hdl.handle.net/10026.1/6502

10.1212/WNL.0000000000002929
Neurology
Ovid Technologies (Wolters Kluwer Health)

Current whole-body MRI applications in the neurofibromatoses

NF1, NF2, and schwannomatosis

Shivani Ahlawat, MD
Laura M. Fayad, MD
Muhammad Shayan Khan, MD
Miriam A. Bredella, MD
Gordon J. Harris, PhD
D. Gareth Evans, MD
Said Farschtschi, MD
Michael A. Jacobs, PhD
Avneesh Chhabra, MD
Johannes M. Salamon, MD
Ralph Wenzel, MD
Victor F. Mautner, MD
Eva Dombi, MD
Wenli Cai, PhD
Scott R. Plotkin, MD, PhD
Jaishri O. Blakeley, MD
On behalf of the Whole Body MRI Committee for the REiNS International Collaboration

Correspondence to Dr. Ahlawat: sahlawa1@jhmi.edu

Supplemental data at Neurology.org

ABSTRACT

Objectives: The Response Evaluation in Neurofibromatosis and Schwannomatosis (REiNS) International Collaboration Whole-Body MRI (WB-MRI) Working Group reviewed the existing literature on WB-MRI, an emerging technology for assessing disease in patients with neurofibromatosis type 1 (NF1), neurofibromatosis type 2 (NF2), and schwannomatosis (SWN), to recommend optimal image acquisition and analysis methods to enable WB-MRI as an endpoint in NF clinical trials.

Methods: A systematic process was used to review all published data about WB-MRI in NF syndromes to assess diagnostic accuracy, feasibility and reproducibility, and data about specific techniques for assessment of tumor burden, characterization of neoplasms, and response to therapy.

Results: WB-MRI at 1.5T or 3.0T is feasible for image acquisition. Short tau inversion recovery (STIR) sequence is used in all investigations to date, suggesting consensus about the utility of this sequence for detection of WB tumor burden in people with NF. There are insufficient data to support a consensus statement about the optimal imaging planes (axial vs coronal) or 2D vs 3D approaches. Functional imaging, although used in some NF studies, has not been systematically applied or evaluated. There are no comparative studies between regional vs WB-MRI or evaluations of WB-MRI reproducibility.

Conclusions: WB-MRI is feasible for identifying tumors using both 1.5T and 3.0T systems. The STIR sequence is a core sequence. Additional investigation is needed to define the optimal approach for volumetric analysis, the reproducibility of WB-MRI in NF, and the diagnostic performance of WB-MRI vs regional MRI. *Neurology*® 2016;87 (Suppl 1):S31–S39

GLOSSARY

ADC = apparent diffusion coefficient; **DWI** = diffusion-weighted imaging; **FDG** = fluorodeoxyglucose; **MPR** = multiplanar reformation; **NF1** = neurofibromatosis type 1; **NF2** = neurofibromatosis type 2; **PNST** = peripheral nerve sheath tumors; **REiNS** = Response Evaluation in Neurofibromatosis and Schwannomatosis; **SNR** = signal to noise ratio; **STIR** = short tau inversion recovery; **SWN** = schwannomatosis; **WB-MRI** = whole-body MRI.

Whole-body MRI (WB-MRI) allows imaging of a large volume of the body in a single image acquisition session. It has been extensively investigated for the detection and staging of visceral and osseous tumors[1–6] and is well-suited to tumor syndromes including neurofibromatosis type 1 (NF1), neurofibromatosis type 2 (NF2), and schwannomatosis (SWN),[7–9] as these patients often have a high burden of tumors as well as large tumors that cross anatomic planes (figure). WB-MRI has been used to evaluate tumor burden and to characterize neoplasms in patients with NF syndromes[10–23] and is being used in some clinical trials to evaluate response to therapy (NCT01207687). A uniform image acquisition protocol and interpretation method would enable WB-MRI to be used as a key endpoint to assess tumor treatment response in multicenter

From The Russell H. Morgan Department of Radiology and Radiological Science (S.A., L.M.F., M.A.J.), Sidney Kimmel Comprehensive Cancer Center (M.A.J.), and Department of Neurology (J.O.B.), Johns Hopkins University, Baltimore, MD; Khyber Medical College (M.S.K.), Peshawar, Pakistan; Department of Radiology (M.A.B., G.J.H., W.C.), Massachusetts General Hospital and Harvard Medical School, Boston; Genomic Medicine (D.G.E.), Manchester Academic Health Science Centre, The University of Manchester, UK; Department of Neurology (S.F., V.F.M.), University Medical Center Hamburg-Eppendorf, Hamburg, Germany; Radiology & Orthopedic Surgery (A.C.), UT Southwestern Medical Center, Dallas, TX; Department of Diagnostic and Interventional Radiology (J.M.S.), University Hospital Hamburg-Eppendorf; Radiological Practice Altona (R.W.), Hamburg, Germany; Pediatric Oncology Branch (E.D.), National Cancer Institute, Bethesda, MD; and Department of Neurology and Cancer Center (S.R.P.), Massachusetts General Hospital, Boston.

REiNS International Collaboration members are listed on the *Neurology*® Web site at Neurology.org.

Go to Neurology.org for full disclosures. Funding information and disclosures deemed relevant by the authors, if any, are provided at the end of the article.

Figure Whole-body MRI in neurofibromatosis

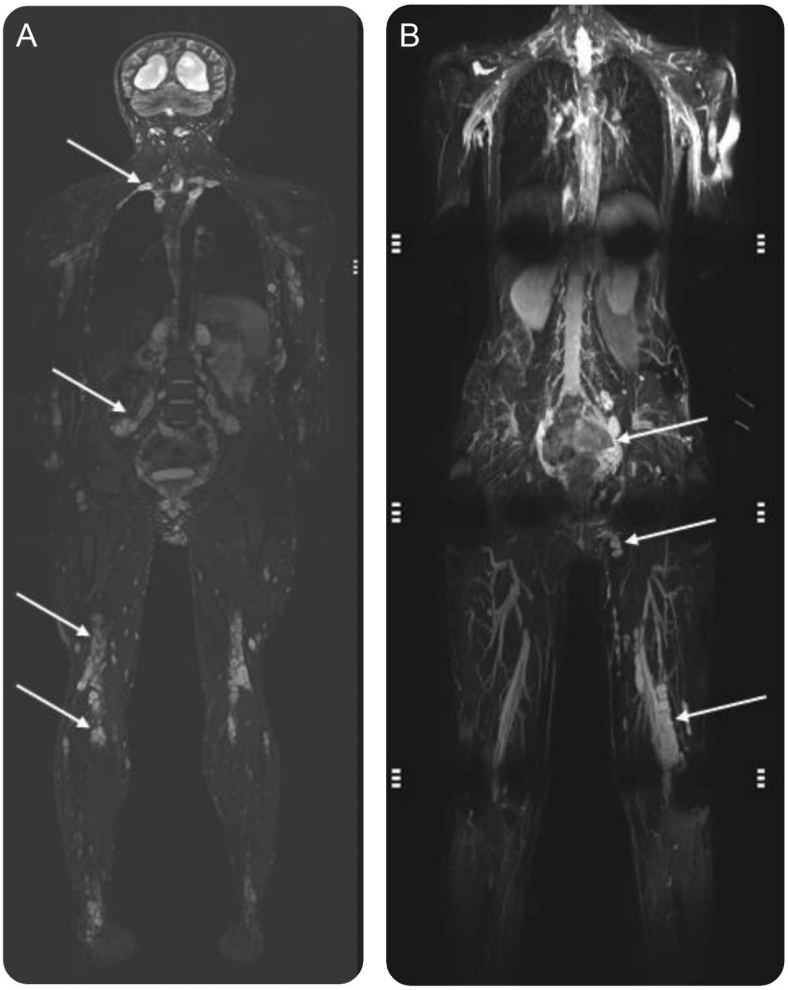

(A) A person with schwannomatosis. (B) A person with neurofibromatosis type 1. In both images, the range of field of view is apparent depending on the table length and the size of the person being imaged and in both images several tumors distributed across anatomic regions can be identified. In (B), some of the artifact that can occur affecting interpretation is apparent.

clinical trials for NF-associated peripheral nerve sheath tumors (PNST). However, thus far, variable approaches have been used for WB-MRI acquisition and image analysis in NF.

The WB-MRI Working Group was formed as part of the Response Evaluation in Neurofibromatosis and Schwannomatosis (REiNS) International Collaboration to generate consensus recommendations and identify priority areas for future research regarding WB-MRI as applied to NF clinical trials. The working group reviewed the existing literature on the use of WB-MRI in patients with NF1, NF2, and SWN to evaluate differences in image acquisition (including magnet strengths, imaging planes, and 2D vs 3D approaches); assess the feasibility, reproducibility, and diagnostic accuracy of WB-MRI in people with NF; and evaluate the benefits of functional MRI techniques, such as diffusion-weighted imaging (DWI) with quantitative apparent diffusion coefficient (ADC) maps and contrast-enhanced imaging for NF-associated PNST. We used this information to recommend best practices for WB-MRI for use in NF clinical trials and to establish research priorities for future studies.

METHODS A computer-aided search of PubMed/MEDLINE from inception to May 2015 was conducted to find relevant English language publications on WB-MRI and NF syndromes. To expand our search, bibliographies of retrieved articles were screened for additional citations. A single reviewer (S.A.) independently screened titles, abstracts, full articles, and references to determine eligibility for inclusion. Studies were included if they had a prospective or retrospective study design with patients of any age with NF1, NF2, and SWN using WB-MRI in which at least the area from the neck to the pelvis was imaged. Review articles, meta-analyses, abstracts, case reports, or case series of less than 10 patients, guidelines, or studies performed in animals were excluded.

Inclusion of patients based on well-established clinical criteria for the NF syndromes was adequate for selection of the patient population, given that pathologic confirmation of each neoplasm is not feasible.[7–9] All included articles were analyzed for diagnosis (NF1, NF2, and SWN), index test (WB-MRI), and reference test (clinical criteria for diagnosis of the NF syndromes). The following information was extracted from articles: author name, year of publication, number of participants, specific tumor syndrome, magnet strength (1.5T vs 3.0T), specific WB-MRI techniques (2D vs 3D imaging, specific imaging sequences, inclusion of functional MRI sequences, contrast administration), sex, mean age with SD, quantification of PNST size (2D vs volumetric), and types of tumors (malignant vs benign PNST). WB-MRI studies were also classified by clinical indication into 3 categories: tumor detection (including extent of disease), tumor characterization, or response to therapy.

RESULTS The literature search yielded 25 articles. After full review of the articles, 14 studies met all inclusion criteria.[10–23] Two studies were excluded as they discussed extratumoral findings (i.e., incidental findings on WB-MRI in NF or marrow changes in patients with NF treated with imatinib mesylate[22,23]). Hence, the final analysis included 12 studies.[10–21]

WB-MRI acquisition protocols. Table 1 summarizes the information extracted from the investigations that met inclusion criteria. Of the 12 publications, 11 employed 1.5T magnet strength[10–12,14–21]; only 1 study used 3.0T magnet.[13] One study performed at 3.0T acquired volumetric 3D images with isotropic resolution in the coronal plane and generated multiplanar reformations (MPR) in sagittal and axial plane with good diagnostic quality.[13] The remainder of the WB-MRI investigations utilized 2D acquisitions in the coronal plane alone, or in both coronal and axial planes. All investigations included a short tau inversion

Table 1	Imaging parameters for WB-MRI from NF-related investigations focused on detection or characterization of PNST			
Publication (see references)	Technical considerations: magnet strength (1.5T vs 3T); sequences (2D vs 3D); plane of acquisition (axial, coronal, sagittal)	Specific sequences	Contrast material (+/−)	Functional DWI and ADC mapping (+/−)
10	1.5T; 2D; coronal	STIR	–	–
11	1.5T; 2D[a]	STIR: slice thickness 5–10 mm; matrix 256–512 × 256; T1; slice thickness 5–10 mm; matrix 256–512 × 256	+; Gadolinium-DTPA (Magnevist, Bayer Schering Pharma AG, Germany)	–
12	1.5T; 2D; coronal	STIR: TR/TE/IR 4,190/111/150; echo train length 25; FOV 50 cm; matrix 320 × 240; slice thickness 10 mm; no interslice gap	–	–
13	3.0T; 3D; coronal	Pre and post contrast VIBE: TR/TE 0.88/2/43 ms; FOV 50 cm^2; matrix 256 × 256; slice thickness 2 mm; STIR: TR/TE 6,640/84 ms; FOV 50 cm^2; matrix 256 × 256; slice thickness 2 mm with interpolation	+; 0.1 mmol/kg gadodiamide contrast agent (Magnevist, Bayer Schering Pharma AG, Germany)	+; TR/TE 4,100/70 ms; b values 50, 400, 800 s/mm^2; FOV 50 cm^2; slice thickness 5 mm
14	1.5T; 2D; coronal and axial	STIR: axial; TR/TE 3,690 ms/106 ms; FOV 25.7 × 50.0 cm; coronal; TR/TE 3,110 ms/101 ms; FOV 48 cm^2; T1W FS pre and post contrast: axial; TR/TE 91 ms/4.76 ms; FOV 47.9 cm^2	0.1 mmol/kg or 0.2 mmol/kg bodyweight gadolinium-DTPA	–
15	1.5T; 2D[a]	STIR: slice thickness 10 mm; no interslice gap	–	–
16	1.5T; 2D; coronal	STIR: TR/TE/IR 4,190/111/150; slice thickness 10 mm; no interslice gap; FOV 50 cm^2; echo train length 25; matrix 320 × 240	–	–
17	1.5T; 2D; axial	STIR: slice thickness 10 mm	–	–
18	1.5T; 2D; axial	STIR: slice thickness 10 mm	–	–
19	1.5T; 2D; coronal	STIR: TR/TE/IR 4,190/111/150; slice thickness 10 mm; no interslice gap; FOV 50 cm^2; echo train length 25; matrix 320 × 240	–	–
20	1.5T; 2D; coronal and axial	Axial: T1 (slice thickness 6–12 mm); T2 FS (slice thickness 6–12 mm); coronal: T1 (slice thickness 5–10 mm); T2 FS (slice thickness 5–10 mm)	–	–
21	1.5T; 2D; coronal and axial	T1SE: slice thickness 5–10 mm; no interslice gap; STIR; slice thickness 5–10 mm; no interslice gap	–	–

Abbreviations: ADC = apparent diffusion coefficient; DWI = diffusion-weighted imaging; FOV = field of view; IR = inversion recovery; NF = neurofibromatosis; PNST = peripheral nerve sheath tumors; STIR = short tau inversion recovery; TE = echo time; TR = repetition time; VIBE = T1-weighted sequences (volume interpolated breath-hold examination); WB-MRI = whole-body MRI.

[a] A plane of imaging is not specified.

recovery (STIR) sequence. Only 1 trial performed functional MRI with quantitative DWI and ADC maps.[13] DWI technique included 3 b values and was performed with slice thickness of 5 mm.[13] Three of the 12 studies used contrast material as an adjunct to traditional WB-MRI fluid-sensitive sequences.[11,13,14] One study obtained postcontrast 3D volumetric gradient echo images[13] while the other study obtained 2D spin echo T1-weighted images with fat suppression.[14] In 1 study, investigators found contrast to be useful in distinguishing PNST from perineural cysts.[13]

WB-MRI applications. With respect to image interpretation and analysis, the following aspects were specifically assessed: tumor detection (evaluation of WB tumor burden, including tumor size), tumor characterization, and the assessment of treatment response (table 2). There are varied methods of WB tumor burden evaluation, with recent studies favoring 3D tumor volumetry, rather than 1D or 2D linear measurements (such as Response Evaluation Criteria in Solid Tumors [RECIST]). Five of the 12 published investigations in this study utilized MedX software (v3.42; Sensor Systems, Inc., Sterling, VA), a semi-automated method for segmentation and measurement with a heuristics-based algorithm for volumetric analysis,[14,15,17,18,21] while 5 of the 12 publications used a computerized 3D-volumetry method developed for WB-MRI using the dynamic threshold level set method.[10–12,16,19] There are limited data with regards to characterization of neoplasms as benign or malignant and no data to date

Table 2 Summary of WB-MRI investigations with respect to image interpretation focused on tumor detection (assessment of whole body tumor burden), characterization, and treatment response

<table>
<tr><th>Reference</th><th>Patient population, n, sex composition (% male), age, y</th><th>Tumor detection (disease burden)</th><th>Conclusion</th></tr>
<tr><td>10</td><td>245 total
<table><tr><th></th><th>NF1</th><th>NF2</th><th>SWN</th></tr><tr><td>N</td><td>142</td><td>53</td><td>50</td></tr><tr><td>%M</td><td>46</td><td>42</td><td>52</td></tr><tr><td>Mean (median) [range]</td><td>38.7 (39) [18–70]</td><td>39.7 (37) [19–76]</td><td>47.6 (44) [25–86]</td></tr></table></td><td><table><tr><th>Median</th><th>NF1</th><th>NF2</th><th>SWN</th></tr><tr><td>Tumor no.</td><td>4</td><td>2</td><td>4</td></tr><tr><td>Tumor volume, mL</td><td>105</td><td>68</td><td>32</td></tr></table>PNST were segmented using computerized 3D-volumetry methods developed for reference 19</td><td>Internal tumor burden is not a primary contributor to QOL but it does correlate with SF-36 bodily pain score</td></tr>
<tr><td>11</td><td>93 (31 NF1 with MPNST and 62 NF1 without MPNST), 58%, median age 34 (range 7–67)</td><td><table><tr><th></th><th>NF1 with MPNST</th><th>NF1 without MPNST</th></tr><tr><td>Mean tumor no.</td><td>2.8</td><td>1.4</td></tr><tr><td>Median volume, mL</td><td>352</td><td>3.8</td></tr></table>PNST were segmented using computerized 3D-volumetry methods developed for reference 19</td><td>Higher number of internal PNs and a greater whole-body PN volume are important risk factors for the development of MPNST</td></tr>
<tr><td>12</td><td>19 (NF1), 52%, mean age 38 (range 19–58)</td><td>Tumor volume range (0.4–1,182.4 mL); PNST were segmented using computerized 3D-volumetry methods developed for reference 19</td><td>NF1 patients with deep tumors and tumors within the trunk are more likely to have metabolically avid (SUVmax greater than 2.5) PNST; increased PNST size, location, and plexiform appearance were associated with increased odds of having a metabolically active PNST</td></tr>
<tr><td>13</td><td>11 (NF2 and SWN)</td><td>23 lesions (median 3.5 cm, range 1.0–10.2 cm); 2/23, cyst; 21/23, PNST</td><td>WB-MRI with volumetric sequences is feasible for detection of PNST in NF; addition of DWI and contrast enables potential for characterization of cysts vs tumors; cysts lack enhancement and have higher ADC values</td></tr>
<tr><td>14</td><td>31, 42%, mean age 30.4 ± 14.7 (range 2–63)</td><td><table><tr><th></th><th>Benign</th><th>Equivocal</th><th>Malignant</th></tr><tr><td>N</td><td>40</td><td>37</td><td>8</td></tr><tr><td>Mean size, cm</td><td>5</td><td>5.9</td><td>5.9</td></tr></table>PNST were segmented using computerized 3D-volumetry methods developed for reference 19</td><td>Although PET/CT has a higher sensitivity on a per lesion basis for characterization of PNST as benign or malignant, addition of WB-MRI may decrease the FP rate</td></tr>
<tr><td>15</td><td>201 (71 with internal PNST), 44%, median age 28.6 (range 1.7–63.4)</td><td><table><tr><th></th><th>Median</th></tr><tr><td>Total body PNST volume</td><td>86.4 mL</td></tr><tr><td>Rate of growth</td><td>3.7%/year</td></tr><tr><td>New PNST in NF1 with >1 tumor on WB-MRI</td><td>0.6%/year</td></tr></table>Volumetry was performed using MedX software (v3.42; Sensor Systems, Sterling, VA), a heuristics-based semi-automated method for segmentation and measurement[36]</td><td>Whole-body PNST volume at the time of the initial WB-MRI correlated with the absolute rate of PNST growth; new PNST are infrequent in patients with NF1 with PNST and unlikely in patients without PNST</td></tr>
<tr><td>16</td><td>247
<table><tr><th></th><th>NF1</th><th>NF2</th><th>SWN</th></tr><tr><td>N</td><td>141</td><td>55</td><td>51</td></tr><tr><td>%M</td><td>47</td><td>42</td><td>51</td></tr><tr><td>Mean age</td><td>38.5</td><td>39.1</td><td>48.5</td></tr></table></td><td>Total of 1,286 PNST (528 plexiform and 758 circumscribed tumors); PNST volume, 65,423 mL in 145/247 patients; PNST were segmented using computerized 3D-volumetry methods developed for reference 19</td><td>Patients with SWN had the highest prevalence of PNST, but patients with NF1 had the highest median tumor volume</td></tr>
<tr><td>17</td><td>38 with large NF1 deletion and 114 age- and sex-matched NF1 patients without large deletion
<table><tr><th></th><th>Mean age ± standard deviation</th></tr><tr><td>Large NF1 deletion</td><td>30.7 ± 14.3</td></tr><tr><td>No large NF1 deletion</td><td>30.7 ± 1.4</td></tr></table></td><td>Internal PNST in 22/38 (58%) deletion and 67/114 (59%) nondeletion patients; volumetry was performed using MedX software (v3.42; Sensor Systems), a heuristics-based semi-automated method for segmentation and measurement[36]</td><td>Patients with NF1 with large deletions have higher internal PNST burden</td></tr>
<tr><td>18</td><td>65 (37 with PNST), 46%, mean 10.5 (range 1.7–17.6)</td><td>73 PNST; mean volume 145.5 mL (excluded PNST < 3 cm); volumetry was performed using MedX software (v3.42; Sensor Systems), a heuristics-based semi-automated method for segmentation and measurement[36]</td><td>PNST can cause clinical deficit in pediatric patients with NF1</td></tr>
<tr><td>19</td><td>52 (NF1: 28, NF2: 14, SWN: 10), 48%, mean age 42 ± 15 (SD) (range 24–86)</td><td>398 Nerve sheath tumors (185 plexiform and 213 discrete tumors) were identified in 29 patients; manual and semi-automated 3D segmented volumetry for 25 plexiform and 25 solitary PNST with high reliability[a]</td><td>DT level set semi-automated segmentation is reliable relative to manual segmentation</td></tr>
<tr><td>20</td><td>24 NF1, 29%, mean and median age 36 (range 15–59)</td><td>4/24, Plexiform; 20/24, solitary; no major problems to differentiate PNST from lymph nodes, vessels, or cysts</td><td>WB-MRI is feasible in NF1 for detection of PNST and assessment of tumor burden</td></tr>
<tr><td>21</td><td>39 (13 NF1 with MPNST and 2 age-/sex-matched NF1 without MPNST), 46%
<table><tr><th></th><th>Median age and range</th></tr><tr><td>NF1 + MPNST</td><td>30 (3–62)</td></tr><tr><td>NF1 − MPNST</td><td>30.5 (2–63)</td></tr></table></td><td><table><tr><th>Median</th><th>NF1 + MPNST</th><th>NF1 − MPNST</th></tr><tr><td>PNST >3cm</td><td>1</td><td>0.5</td></tr><tr><td>Tumor volume</td><td>427</td><td>5</td></tr></table>Volumetry using MEDx software platform[37]</td><td>WB-MRI enables detection of internal PNST burden</td></tr>
</table>

Abbreviations: ADC = apparent diffusion coefficient; DWI = diffusion-weighted imaging; FP = false positive; MPNST = malignant peripheral nerve sheath tumor; NF1 = neurofibromatosis type 1; NF2 = neurofibromatosis type 2; PN = peripheral nerve; PNST = peripheral nerve sheath tumors; QOL = quality of life; SF-36 = Short Form-36; SWN = schwannomatosis; WB-MRI = whole-body MRI.

[a] Segmented using computerized 3D-volumetry methods developed for WB-MRI using (the dynamic threshold [DT] level set method).

Table 3 Future directions for whole-body MRI (WB-MRI) investigations in patients with neurofibromatosis (NF)
Sensitivity, specificity, and reproducibility of WB-MRI in NF
1. Comparative study of 3.0T vs 1.5T for tumor detection
2. Comparative study for 2D vs 3D acquisition for tumor detection
3. Comparative study of axial vs coronal imaging acquisition for tumor detection
4. Comparative study of regional vs WB-MRI for tumor detection
5. Test retest variability and interobserver performance of WB-MRI in NF
6. Determination of the minimally meaningful clinical change of tumor size with WB-MRI
Biologic characterization of tumor
1. Investigate functional MRI (diffusion-weighted imaging/apparent diffusion coefficient mapping) vs other imaging modalities such as fluorodeoxyglucose PET for tumor characterization and assessment of treatment response
2. Investigate the added value of contrast-enhanced imaging to WB-MRI protocol for characterization and assessment of treatment response

for assessment of treatment response, although such analysis is ongoing in a clinical trial assessing WB-MRI over time in people with NF2 treated with bevacizumab (NCT01207687).

The data from tables 1 and 2 were critically evaluated to generate knowledge gaps and future directions for WB-MRI investigations to provide the required metrics for inclusion of WB-MRI as a primary endpoint in clinical trials for NF-associated PNST. Priority areas identified include WB-MRI reproducibility for anatomical measures, optimal analysis techniques, and establishing the minimal meaningful clinical difference in tumor size (table 3).

DISCUSSION WB-MRI provides continuous coverage of lesions that cross anatomical boundaries and therefore cannot be fully imaged with localized MRI, a significant advantage when evaluating patients with NF syndromes where there are frequently large infiltrative tumors (figure) or multifocal PNST, which may be missed without WB-MRI assessment.[21] In this setting, WB-MRI allows assessment of differential response within and across tumors over time. An additional advantage is that WB-MRI can be completed with a typical scan time of 45–60 minutes on both 1.5T and 3.0T systems and uses the same protocols for patients of all ages, allowing continuity across and within patients enrolled in a therapeutic trial.[12,13,18]

A major goal of this work was to identify core aspects of WB-MRI application for assessment of NF-associated PNST to enable inclusion of WB-MRI as a primary endpoint for therapeutic trials of NF-associated PNST. There are no comparative data available with respect to magnet strength, image acquisition plane (axial vs coronal), 2D or 3D acquisition, or the value of functional imaging and administration of contrast material available across all available investigations. However, after the analyses of the WB-MRI studies in patients with NF conducted to date, several statements can be made: WB-MRI in NF is feasible both at 1.5T or 3.0T; it can be standardized across multiple sites for anatomic tumor assessment in the setting of a clinical trial; both 2D and 3D acquisition are operational for generating tumor data; STIR is a core sequence for evaluation of tumor burden; and functional sequences such as DWI can be considered in the setting of WB-MRI. Outside of these statements, the WB-MRI Working Group of REiNS is not able to make specific recommendations for acquisition protocols at this time due to a lack of data. For example, only a single case series of 4 patients compared analysis of tumor burden in patients with NF1 who underwent WB-MRI on both 1.5T and 3.0T within a 6-month period.[24] This study showed no difference in tumor volumes between the 2 magnet strengths; however, there are no other comparative analyses and this study is too small to draw conclusions. The majority of studies completed to date use 1.5T as this is more widely available. The wide availability of 1.5T magnets is an advantage for application of WB-MRI to multicenter trials. However, 3.0T WB-MRI has theoretical advantages, such as increased signal to noise ratios (SNR), allowing for improved 3D sequences as well as allowing for DWI acquisition in an acceptable imaging time. Potential disadvantages of 3.0T MRI include B1 field inhomogeneities and susceptibility artifacts.[2,13] Work is ongoing to optimize this with technological advances such as continuous table motion and improved coils, which are expected to shorten acquisition and increase SNR.[2,25]

With respect to specific sequences, the STIR sequence, with its combined T1 and T2 weighting, has been uniformly used in the WB-MRI investigations for PNST. Most pathologic processes, including tumors, are proton-rich with resultant prolonged T1 and T2 relaxation times and increased signal intensity on STIR images. In addition, fat suppression is more robust and homogeneous on inversion recovery sequences than other frequency selective sequences. These features make the STIR sequence valuable for detection and measurement of PNST and a core sequence for assessment of whole body tumor burden in NF. However, detection of other pathologies in the viscera or the skeletal system may require additional imaging.

Regarding 2D and 3D acquisitions, 11 of the 12 studies used 2D imaging sequences,[10–12,14–21] while only 1 study (at 3.0T) obtained images with 3D volumetric sequences.[13] This allows us to say that both are feasible, but there are no data to suggest advantages of one over the other. There are important differences in spatial resolution between 2D and 3D sequences. For 2D sequences obtained at 1.5T, the in-plane resolution can be 0.3–1.5 mm and the slice thickness can range from 5 to 10 mm with no interslice gap. WB-MRI at this resolution may not be adequate for the detection or characterization of very small neoplasms and PNST located in the skin and subcutaneous tissues. 3D sequences obtained at 3.0T can have an interpolated spatial resolution of 2 mm with slice thickness of 2 mm and no interslice gap.[13] Both 2D and 3D sequences can also be performed with higher spatial resolution, but at the cost of longer acquisition time. A potential advantage of 3D sequences includes MPR capabilities such that a 3D isotropic dataset can be displayed in any imaging plane. However, 3D acquisition may not be available on all scanners, limiting application in multicenter studies.

For both 2D and 3D sequences, there is a lack of consensus regarding an optimal imaging plane. Although all WB-MRI investigations to date have included the coronal plane, no comparative study has been performed to determine the ideal imaging plane. An advantage of coronal image acquisition is that for anatomic sequences such as STIR or T1-weigted imaging, there is less respiratory motion due to faster image acquisition. Of note, the coronal image acquisition may not be optimal for DWI, particularly in the neck and thoracic regions, due to cardiac motion.

There is also a lack of data regarding the added value of IV contrast material. Use of exogenous contrast requires venous access and hemodynamic monitoring during the WB-MRI acquisition that may reduce feasibility and carries the additional risk of nephrogenic systemic fibrosis in the setting of renal failure. New literature also suggests a relationship between repetitive gadolinium exposure and high signal intensity in the basal ganglia, further raising concern about exogenous contrast.[26] There are currently insufficient data to assess the potential diagnostic benefit vs risk of the use of IV contrast for PNST. Finally, no investigations have been performed to assess the added value of DWI with ADC maps to standard sequences in WB-MRI in patients with NF. This is feasible and the potential advantages include the assessment of tumor biology and possibly treatment response, the ability to distinguish a cyst from a neoplasm, and the characterization of incidental findings. For example, specific threshold ADC values enable distinguishing soft tissue masses from cysts with high specificity (100%), important when quantifying tumor burden.[13,27] Similarly, there is localized MRI experience using DWI and ADC mapping for PNST characterization as benign or malignant with 100% sensitivity (95% confidence interval 66.4%–100%) and 77% specificity.[28] There is also limited experience comparing WB-MRI with whole body 18F-fluorodeoxyglucose (FDG) PET/CT for characterizing PNST as benign or malignant.[14] Although 18F-FDG PET/CT had higher sensitivity (100%) compared with WB-MRI (66.7%) on a per lesion basis, WB-MRI had a higher specificity (97% for WB-MRI vs 74.4% for 18F-FDG PET/CT) for detecting malignancy.[14] WB-MRI in this particular investigation used routine anatomic sequences only,[14] and thus it remains to be determined whether addition of quantitative functional MRI sequences with ADC measurements would alter the diagnostic accuracy for detection of malignancy.

Although WB-MRI with functional sequences for detection and characterization of benign vs malignant PNST shows promise, currently these sequences can be difficult to perform uniformly across multiple sites. No investigations have been published to date regarding the assessment of treatment response in PNST in NF, but there are efforts currently for analysis of ongoing therapeutic studies with pretreatment and posttreatment WB-MRI (NCT01207687). This study will also allow assessment of the added value of functional MRI or contrast-enhanced sequences for assessing changes in tumor biology independent of changes in tumor size.

With respect to WB-MRI analysis, the field has recommended volumetric measurements of tumor rather than 2D measures.[29–31] Tumor volumetry is preferred for quantifying complex PNST such as plexiform neurofibromas that can be large and infiltrative whereas 2D or linear measurement is more likely to misrepresent the true tumor dimensions by overestimating or underestimating PNST size and can be fraught with interobserver and intraobserver variations.[32–34] Tumor volumetry, particularly in infiltrative plexiform neoplasms such as the ones identified in patients with NF syndromes, has become the optimal approach for assessing tumor burden. In addition, the current therapeutic trials in NF syndromes use volumetric analysis as a primary or secondary endpoint (NCT01362803, NCT02101736, NCT02096471). Volumetric tumor burden can be measured manually, though this is time-consuming and impractical for routine clinical evaluation. Computer-aided tumor segmentation of PNST can be performed on MRI sequences that show clear distinction between tumor and surrounding normal tissue, such as STIR or similar fluid sensitive sequences. In one study comparing manual and semi-automated tumor volumetry, computerized volumetry using a dynamic threshold method was superior to manual segmentation techniques.[19] Moreover, computerized volumetry was reliable and less labor intensive, which made it more repeatable compared to manual segmentation.[19] It is important to note that reliability and repeatability were calculated using a small sample size[19]; however, this technique has subsequently been applied in larger studies of approximately 250 patients.[10–12] A multicenter study comparing the 2 principal semi-automated methods for reliability and interpretation time compared with the manual technique in lesion detection and change in lesion size is currently underway.

Although there are several advantages to WB-MRI for NF, there are also important limitations. First, for very tall or large individuals, portions of the body may not be adequately imaged, including the distal legs, shoulders, and arms. Adequate imaging of the distal lower extremities is a particular concern for 3.0T scanners and may limit the use of WB-MRI if there are tumors of interest in these regions. This can be addressed by imaging the upper and lower body separately; however, this increases cost and time. An additional concern for tumor assessment with WB-MRI is that the lower limit of tumor volume that can be assessed has not been described, and depending on the WB-MRI technique as well as the tumor distribution, the cutoff value may be variable. Selecting the same PNST for contouring consistently over consecutive scans is crucial for determining size change and can only be done on comparable quality image sets. Similarly, diagnostic performance of WB-MRI for total tumor burden estimates is dependent on the correct representation of the body on the MRI and needs to be standardized across sites and time points. Importantly, WB-MRI can suffer from varied image distortions at the periphery of the imaging field, which may lead to measurement errors.[13] Given spatial resolution limitations and depending on what sequences are applied, additional dedicated MRI sequences such as magnetic resonance neurography may be necessary to provide improved anatomic and functional characterization of PNST,[35] evaluate tumors in and around the spinal cord, identify small tumors such as pheochromocytomas, or diagnose vascular anomalies. Finally, it is worth noting that there are some limitations to the analysis presented based on the very limited literature on this topic. Only 14 investigations fulfilled search criteria. Of these, several studies had overlapping patient data and WB-MRI protocols reported with separate endpoints.[10,16,19] This further highlights the need for additional research on WB-MRI performance in NF syndromes (table 3).

Choosing standardized image acquisition and analysis methods is essential for optimal multicenter collaboration applying WB-MRI as a tool for assessing tumors in NF. WB-MRI may serve as either a primary or secondary endpoint in clinical drug trials that target multiple tumors requiring systemic rather than localized imaging. The systematic process developed by the REiNS WB-MRI Working Group has enabled a multicenter conversation about imaging protocols and the development of future comparative projects. These results will be used by the group to identify the most appropriate WB-MRI acquisition and interpretation methods for individuals with NF syndromes in future clinical trials and prioritize research questions about the optimal use of WB-MRI as an endpoint measure in NF research.

AUTHOR CONTRIBUTIONS

S. Ahlawat: conceptualization of the study, interpretation of the data, drafting the manuscript. L.M. Fayad: conceptualization of the study, interpretation of the data, drafting the manuscript. S. Khan: analysis of the data. M.A. Bredella: revising the manuscript for intellectual content. G.J. Harris: revising the manuscript for intellectual content. D.G. Evans: revising the manuscript for intellectual content. S. Farschtschi: analysis of the data, revising the manuscript for intellectual content. M.A. Jacobs: analysis of the data, revising the manuscript for intellectual content. A. Chhabra: revising the manuscript for intellectual content. J.M. Salamon: revising the manuscript for intellectual content. R. Wenzel: analysis of the data, revising the manuscript for intellectual content. V.F. Mautner: revising the manuscript for intellectual content. E. Dombi: conceptualization of the study, interpretation of the data, revising the manuscript for intellectual content. W. Cai: interpretation of the data, revising the manuscript for intellectual content. S.R. Plotkin: conceptualization of the study, interpretation of the data, revising the manuscript for intellectual content. J.O. Blakeley: conceptualization of the study, interpretation of the data, drafting the manuscript.

ACKNOWLEDGMENT

The authors thank Rhonda Jackson and Monica R. Sheridan for administrative support.

STUDY FUNDING

No targeted funding reported.

DISCLOSURE

S. Ahlawat reports no disclosures relevant to the manuscript. L. Fayad has received research grants from General Electric Radiology Research Academic Fellowship program and Siemens Medical Systems. M. Khan and M. Bredella report no disclosures relevant to the manuscript. G. Harris receives research support from Children's Tumor Foundation and NIH. He also serves on the scientific advisory board of Fovia, Inc. G. Evans received support from AstraZeneca and has served on the board of *Familial Cancer Journal*. S. Farschtschi reports no disclosures relevant to the manuscript. M. Jacobs receives funding from NIH (P50CA103175, 5P30CA006973 [IRAT], R01CA190299, U01CA140204) and Siemens Medical Systems (JHU-2012-MR-86-01). A. Chhabra has received research grants from General Electric Radiology Research Academic Fellowship program, Siemens Medical Solutions, Gatewood Fellowship Award, and Integra Life Sciences. He also serves as a research consultant with Siemens CAD group. He receives royalties from Wolters and Jaypee Publishers. J. Salamon, R. Wenzel, V. Mautner, and E. Dombi report no disclosures relevant to the manuscript. W. Cai receives research support from NCI, American Cancer Society, and Children's Tumor Foundation. He serves on the editorial boards of the *International Journal of Intelligent Information Processing*, *World Journal of Radiology*, *International Journal of Radiology*, and *Advances in Modern Oncology Research*. S. Plotkin receives research support from the Children's Tumor Foundation, NIH, and the Department of Defense Neurofibromatosis Clinical Trials Consortium. J. Blakeley has received research support from GlaxoSmithKline, Sanofi-Aventis, and Lily Pharmaceuticals. She has consulted for Abbvie. Go to Neurology.org for full disclosures.

Received November 19, 2015. Accepted in final form May 26, 2016.

REFERENCES

1. Toledano-Massiah S, Luciani A, Itti E, et al. Whole-body diffusion-weighted imaging in Hodgkin lymphoma and diffuse large B-cell lymphoma. Radiographics 2015;35:747–764.
2. Pasoglou V, Michoux N, Peeters F, et al. Whole-body 3D T1-weighted MR imaging in patients with prostate cancer:

feasibility and evaluation in screening for metastatic disease. Radiology 2015;275:155–166.
3. Friedman DN, Lis E, Sklar CA, et al. Whole-body magnetic resonance imaging (WB-MRI) as surveillance for subsequent malignancies in survivors of hereditary retinoblastoma: a pilot study. Pediatr Blood Cancer 2014;61: 1440–1444.
4. Ciliberto M, Maggi F, Treglia G, et al. Comparison between whole-body MRI and fluorine-18-fluorodeoxyglucose PET or PET/CT in oncology: a systematic review. Radiol Oncol 2013;47:206–218.
5. Schlemmer HP, Schäfer J, Pfannenberg C, et al. Fast whole-body assessment of metastatic disease using a novel magnetic resonance imaging system: initial experiences. Invest Radiol 2005;40:64–71.
6. Attariwala R, Picker W. Whole body MRI: improved lesion detection and characterization with diffusion weighted techniques. J Magn Reson Imaging 2013;38: 253–268.
7. Mulvihill JJ, Parry DM, Sherman JL, Pikus A, Kaiser-Kupfer MI, Eldridge R. NIH conference: neurofibromatosis 1 (Recklinghausen disease) and neurofibromatosis 2 (bilateral acoustic neurofibromatosis): an update. Ann Intern Med 1990;113:39–52.
8. Baser ME, Friedman JM, Wallace AJ, Ramsden RT, Joe H, Evans DG. Evaluation of clinical diagnostic criteria for neurofibromatosis 2. Neurology 2002;59:1759–1765.
9. MacCollin M, Chiocca EA, Evans DG, et al. Diagnostic criteria for schwannomatosis. Neurology 2005;64:1838–1845.
10. Merker VL, Bredella MA, Cai W, et al. Relationship between whole-body tumor burden, clinical phenotype, and quality of life in patients with neurofibromatosis. Am J Med Genet A 2014;164A:1431–1437.
11. Nguyen R, Jett K, Harris GJ, Cai W, Friedman JM, Mautner VF. Benign whole body tumor volume is a risk factor malignant peripheral nerve sheath tumors in neurofibromatosis type 1. J Neurooncol 2014;116:307–313.
12. Urban T, Lim R, Merker VL, et al. Anatomic and metabolic evaluation of peripheral nerve sheath tumors in patients with neurofibromatosis 1 using whole-body MRI and (18)F-FDG PET fusion. Clin Nucl Med 2014;39: e301–e307.
13. Fayad LM, Blakeley J, Plotkin S, Widemann B, Jacobs MA. Whole body MRI at 3T with quantitative diffusion weighted imaging and contrast-enhanced sequences for the characterization of peripheral lesions in patients with neurofibromatosis type 2 and schwannomatosis. ISRN Radiol 2013;2013:627932.
14. Derlin T, Tornquist K, Münster S, et al. Comparative effectiveness of 18F-FDG PET/CT versus whole-body MRI for detection of malignant peripheral nerve sheath tumors in neurofibromatosis type 1. Clin Nucl Med 2013; 38:e19–e25.
15. Nguyen R, Dombi E, Widemann BC, et al. Growth dynamics of plexiform neurofibromas: a retrospective cohort study of 201 patients with neurofibromatosis 1. Orphanet J Rare Dis 2012;7:75.
16. Plotkin SR, Bredella MA, Cai W, et al. Quantitative assessment of whole-body tumor burden in adult patients with neurofibromatosis. PLoS One 2012;7:e35711.
17. Kluwe L, Nguyen R, Vogt J, et al. Internal tumor burden in neurofibromatosis type I patients with large NF1 deletions. Genes Chromosomes Cancer 2012;51:447–451.
18. Nguyen R, Kluwe L, Fuensterer C, Kentsch M, Friedrich RE, Mautner VF. Plexiform neurofibromas in children with neurofibromatosis type 1: frequency and associated clinical deficits. J Pediatr 2011;159:652–655.e2.
19. Cai W, Kassarjian A, Bredella MA, et al. Tumor burden in patients with neurofibromatosis types 1 and 2 and schwannomatosis: determination on whole-body MR images. Radiology 2009;250:665–673.
20. Van Meerbeeck SF, Verstraete KL, Janssens S, Mortier G. Whole body MR imaging in neurofibromatosis type 1. Eur J Radiol 2009;69:236–242.
21. Mautner VF, Asuagbor FA, Dombi E, et al. Assessment of benign tumor burden by whole-body MRI in patients with neurofibromatosis 1. Neuro Oncol 2008;10:593–598.
22. Jaremko JL, MacMahon PJ, Torriani M, et al. Whole-body MRI in neurofibromatosis: incidental findings and prevalence of scoliosis. Skeletal Radiol 2012;41:917–923.
23. Karmazyn B, Cohen MD, Jennings SG, Robertson KA. Marrow signal changes observed in follow-up whole-body MRI studies in children and young adults with neurofibromatosis type 1 treated with imatinib mesylate (Gleevec) for plexiform neurofibromas. Pediatr Radiol 2012;42:1218–1222.
24. Farschtschi SC, Dombi E, Widemann B, Fünsterer C, Mautner VF. Comparability of 1.5T and 3.0T MRI-volumetrics in neurofibromatosis type 1. Presented at the 2013 NF Conference, Monterey, CA.
25. Brauck K, Zenge MO, Vogt FM, et al. Feasibility of whole-body MR with T2- and T1-weighted real-time steady-state free precession sequences during continuous table movement to depict metastases. Radiology 2008; 246:910–916.
26. Kanda T, Ishii K, Kawaguchi H, Kitajima K, Takenaka D. High signal intensity in the dentate nucleus and globus pallidus on unenhanced T1-weighted MR images: relationship with increasing cumulative dose of a gadolinium-based contrast material. Radiology 2014;270:834–841.
27. Subhawong TK, Durand DJ, Thawait GK, Jacobs MA, Fayad LM. Characterization of soft tissue masses: can quantitative diffusion weighted imaging reliably distinguish cysts from solid masses? Skeletal Radiol 2013;42: 1583–1592.
28. Demehri S, Belzberg A, Blakeley J, Fayad LM. Conventional and functional MR imaging of peripheral nerve sheath tumors: initial experience. AJNR 2014;35:1615–1620.
29. Dombi E, Ardern-Holmes SL, Babovic-Vuksanovic D, et al. Recommendations for imaging tumor response in neurofibromatosis clinical trials. Neurology 2013;81(21 suppl 1): S33–S40.
30. Widemann BC, Blakeley JO, Dombi E, et al. Conclusions and future directions for the ReiNS International Collaboration. Neurology 2013;81(21 suppl 1):S41–S44.
31. Harris GJ, Plotkin SR, MacColllin M, et al. Three-dimensional volumetrics for tracking vestibular schwannoma growth in neurofibromatosis type II. Neurosurgery 2008; 62:1314–1319.
32. Hopper KD, Kasales CJ, Van Slyke MA, Schwartz TA, TenHave TR, Jozefiak JA. Analysis of interobserver and intraobserver variability in CT tumor measurements. AJR Am J Roentgenol 1996;167:851–854.
33. Dempsey MF, Condon BR, Hadley DM. Measurement of tumor "size" in recurrent malignant glioma: 1D, 2D, or 3D? AJNR Am J Neuroradiol 2005;26:770–776.
34. Erasmus JJ, Gladish GW, Broemeling L, et al. Interobserver and intraobserver variability in measurement of non-small-

cell carcinoma lung lesions: implications for assessment of tumor response. J Clin Oncol 2003;21:2574–2582.
35. Chhabra A, Thakkar RS, Andresisek G, et al. Anatomic MR imaging and functional diffusion tensor imaging of peripheral nerve tumors and tumorlike conditions. AJNR Am J Neuroradiol 2013;34: 802–807.
36. Solomon J, Warren K, Dombi E, Patronas N, Widemann B: Automated detection and volume measurement of plexiform neurofibromas in neurofibromatosis 1 using magnetic resonance imaging. Comput Med Imaging Graph 2004;28:257–265.
37. Dombi E, Solomon J, Gillespie AJ, et al. NF1 plexiform neurofibroma growth rate by volumetric MRI: relationship to age and body weight. Neurology 2007;68:643–647.

Neurology®

Current whole-body MRI applications in the neurofibromatoses: NF1, NF2, and schwannomatosis

Shivani Ahlawat, Laura M. Fayad, Muhammad Shayan Khan, et al.
Neurology 2016;87;S31-S39
DOI 10.1212/WNL.0000000000002929

This information is current as of August 15, 2016